IEEE Access
Multidisciplinary ⋮ Rapid Review ⋮ Open Access Journal

Received September 10, 2021, accepted October 4, 2021, date of publication October 6, 2021, date of current version October 13, 2021.

Digital Object Identifier 10.1109/ACCESS.2021.3118606

Trapping Nanoparticles Using Localized Surface Plasmons of Graphene Nanodisks

ALI ASGHAR KHORAMI[1], MOHAMMAD MAHDI ABBASI[1], AND ATHAR SADAT JAVANMARD[2]
[1]Nanoelectronics Group, Department of Engineering, Tarbiat Modares University, Tehran 1411713116, Iran
[2]Department of Biology, Faculty of Science, Yasouj University, Yasuj 7591874934, Iran

Corresponding authors: Ali Asghar Khorami (aa.khorami@modares.ac.ir) and Mohammad Mahdi Abbasi (m.abbasi63@modares.ac.ir)

ABSTRACT Given the sub-wavelength trapping challenges in the optical tweezers, the plasmonic tweezers serve as a bridge by breaking the diffraction limit. Hence, the development of plasmonic tweezers can open up many potential applications in biology, medicine, and chemistry. In this paper, using localized surface plasmons (LSPs) of graphene nanodisk with a resonance frequency of 20 THz, we design a lab-on-a-chip optophoresis system, which can be utilized to effectively trap the nanoparticles. The LSPs of graphene nanodisk generate a large field gradient in the deep sub-wavelength area around the resonance frequency. We show that by an appropriate choice of chemical potentials of the graphene nanodisks, the strong optical near-field forces desired for trapping can be generated under the illumination of the THz source when the polystyrene (PS) nanoparticles are located in the vicinity of graphene nanodisks. Numerical simulations show that the designed system with graphene nanodisks of 250 nm in diameter and chemical potentials of $\mu_c = 0.6$ eV can trap the PS nanoparticles of 12 nm in diameter and larger with a THz source intensity of 19 $mW/\mu m^2$, demonstrating acceptable sensitivities for variations in the nanoparticle diameter and refractive index. Moreover, at the same source intensity, the graphene nanodisks with $\mu_c = 0.7$ eV can trap the PS nanoparticle as small as 9.5 nm in diameter.

INDEX TERMS Localized surface plasmons, plasmonic tweezers, graphene, nanodisk.

I. INTRODUCTION

Optical tweezing has become a noninvasive manipulation method mainly in biology, chemistry, and nano-science [1]. Nevertheless, the manipulation of nanoparticles in the Rayleigh regime still remains a challenging task because it is rather difficult to perform stable optical trapping as the size of the particle gets smaller [2], [3]. Plasmonic nanostructures can overcome this limitation and allow the manipulation of optical fields on deep sub-wavelength scales [4]–[8]. Several types of metallic nanostructures such as nanoantennas [9]–[12], nanohole apertures [13]–[16], and flat particles [17] have been used for plasmonic trapping. However, the significant loss in metals and consequent heat generation that may damage the biological tissues are the major drawback of using metal-dielectric interfaces for plasmonic trapping [18], [19]. Nevertheless, researchers have shown that graphene due to its exceptional electrical, mechanical, thermal, and optical properties can be an outstanding material for plasmonic applications [20]–[25]. Besides, the biocompatibility nature of graphene makes it a very promising candidate for applications in biology, chemistry, and medicine [26], [27]. Compared with plasmons in noble metals, the graphene plasmons exhibit extraordinarily strong optical confinement and long lifetimes due to the high mobility of carriers in graphene [28]–[30]. Besides, the plasmon's field intensity can be controlled by changing the chemical potential of graphene at an appropriate fixed incident laser power [31]–[33]. Furthermore, the high thermal conductivity of graphene as compared with metals, causes the heat absorbed from the incident beam to be removed efficiently, which is vital for manipulating biological samples [34]. On the other hand, because of the opaqueness of the metal surface, the observation of the particles in metal-based plasmonic tweezers is a challenge that can be solved through the use of graphene in place of metal. Because it is a thin film transparent to light [35]. Therefore, due to the relatively low loss, remarkable enhancement of local electromagnetic fields, high confinement, and tunability, graphene can be a superior alternative plasmonic material to noble metals.

The associate editor coordinating the review of this manuscript and approving it for publication was Derek Abbott.

Recently, a few numbers graphene structures such as hole [35], [36], sheet [31], [37], ribbon [32], and ring [33] have been used for plasmonic trapping and this field is growing. In this paper, using the unique properties of graphene plasmons, we present a novel structure based on the graphene nanodisks for trapping the nanoparticles. Although the infrared photodetectors based on graphene nanodisks have been reported [38]–[41], to date, the trapping capability of graphene nanodisks has not been investigated in the literature. Here, we investigate the trapping capabilities of 2-dimensional arrays of graphene nanodisks with appropriate diameters and chemical potentials. The proposed plasmonic tweezer system, benefiting from low energy consumption and the outstanding properties of graphene plasmon, is capable of trapping nanoparticles with acceptable sensitivities for variations in the nanoparticle diameter and refractive index.

II. PROPOSED STRUCTURE AND OPERATION PRINCIPLE

We investigate a 2-dimensional (2D) periodic system that can be employed for trapping the nanoparticles. Fig. 1 (a) illustrates a three-dimensional (3D) schematic of the proposed plasmonic tweezer. It is composed of a 2D array of graphene nanodisks. The period of the graphene nanodisk array is $P_X = P_y = 450$ nm, and the diameter of the nanodisks is $D = 250$ nm. The underlying substrate is a Si wafer covered with a 100 nm thin layer of SiO_2. An appropriate microfluidic channel, filled with water as a typical fluid used in tweezer systems [42], [43], is devised on the top of the structure. As depicted in Fig. 1 (a), the polystyrene nanoparticles with different diameters (d) suspended in water are injected into the microfluidic channel by a syringe similar to those of [44], [45]. Moreover, the sheath flows help most of the injected nanoparticles to move above the graphene nanodisks, as trapping centers. Fig. 1 (b) illustrates a cross-section view of the proposed plasmonic tweezer, in the x-z plane.

Before going any further, we briefly explain the operation principle of the proposed system. Consider a plane wave single-mode THz source with its electric field polarized along the x-direction that is illuminated on the graphene nanodisks at normal incidence. At the resonance frequency, the LSPs of graphene nanodisks can be strongly excited. The LSPs lead to strong optical field gradients around the edges of graphene nanodisks. A nanoparticle positioned near this LSPs field above the surface of a graphene nanodisk may experience an optical force. The out-of-plane component of the gradient force can be balanced by various opposing forces, originating from the fluidic lift, thermophoresis, gravity, and electrostatic mechanisms, preventing the particles from sticking to the nanodisk surface [46]. The in-plane component of the gradient force excreted on the nanoparticles due to the highly confined LSPs field can trap the nanoparticles if satisfied trapping condition. Otherwise, the nanoparticles are unaffected by the plasmonic force and under the influence of the fluid driving force continue to move out from the outlet. Note

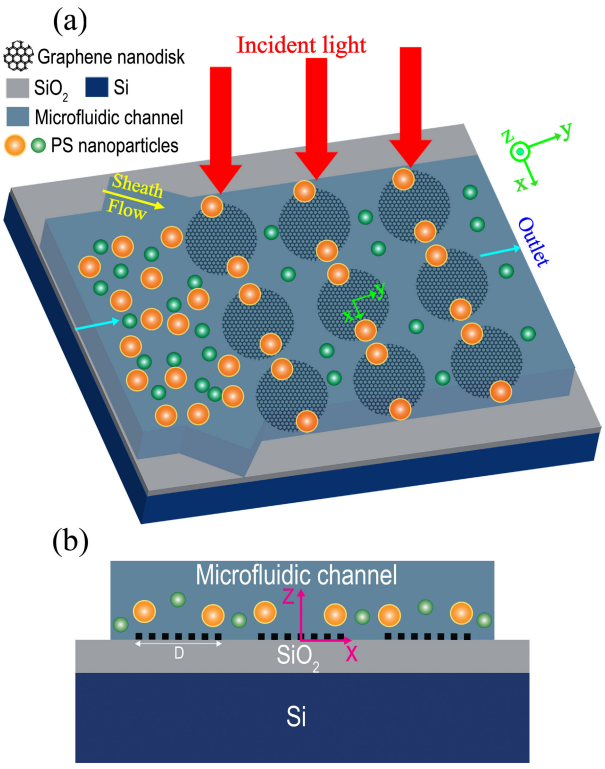

FIGURE 1. (a) A 3D schematic view of the proposed plasmonic tweezer based on graphene nanodisks. (b) A cross-section view of the proposed plasmonic tweezer, in the x-z plane.

that, the threshold for the stable trapping potential energy is $-10\,K_BT$, wherein k_B and T are the Boltzmann constant and the ambient temperature, respectively.

III. THEORY BEHIND THE TRAPPING

To determine the total induced optical force on a nanoparticle, we use the Maxwell stress tensor (MST) method. So that the average optical force exerted on a nanoparticle interacting with an electromagnetic field is given by [47], [48]:

$$< F > = \frac{1}{2} Re \oint_{\Omega} T(r,t).n\, dS \tag{1}$$

where,

$$\begin{aligned} T(r,t) = {} & \varepsilon E(r,t) \otimes E^*(r,t) \\ & + \mu H(r,t) \otimes H^*(r,t) \\ & - \frac{1}{2}(\varepsilon |E(r,t)|^2 + \mu |H(r,t)|^2) \end{aligned} \tag{2}$$

is the Maxwell stress tensor, n is the unit vector normal to the surface S enclosing the particle volume Ω, r and t are the position vector and time, ε and μ are the medium permittivity and permeability, and E and H are the electric and the magnetic field vectors, respectively.

The trapping potential comes from the gradient force that determines the stability of the trap, can be obtained from [49]:

$$U(r_0) = -\int_{\infty}^{r_0} F(r).\, dr \tag{3}$$

In the case where there exists a significant gradient in the intensity of the light field such as in the evanescent field of LSPs, the gradient force (F_{grad}) takes the form shown below [3], [50]:

$$F_{grad} = \frac{6\pi V(\varepsilon_p - \varepsilon_w)}{c(\varepsilon_p + 2\varepsilon_w)}\nabla I \tag{4}$$

where $V = (\frac{4}{3})\pi R^3$ is the nanoparticle volume, R is the radius of the dielectric particle, c is the speed of light in vacuum, I is the intensity, ε_p and ε_w are the relative permittivity of a dielectric particle and water, respectively.

The potential energy experienced by a dielectric particle that is suspended in the water solution, at a point in the given plane, can be simplified to [3], [29], [50]:

$$U(r) = -\frac{\pi^2 d^3(\varepsilon_p - \varepsilon_w)}{c(\varepsilon_p + 2\varepsilon_w)}I \tag{5}$$

where d is the diameter of a dielectric particle.

As can be seen in (3), the potential energy is obtained by integrating force. According to (1) and (2), the force depends on the plasmon's field. The plasmon's field comes from the excitation of LSPs on the surface of graphene nanodisk and it depends on the nanodisk diameter, chemical potential, relative permittivity, and optical conductivity of graphene nanodisk.

The relative permittivity of graphene has the following form [26], [29], [51], [52]:

$$\varepsilon_g(\omega) = \frac{(\varepsilon_w + \varepsilon_{substrate})}{2} + i\frac{\sigma(\omega)}{\varepsilon_0\omega\Delta} \tag{6}$$

where graphene is surrounded by materials with dielectric constants ε_w and $\varepsilon_{substrate}$. ε_0 is the permittivity of free space, ω is the angular frequency, $\Delta = 0.34$ nm is the graphene thickness, and σ is the optical conductivity of the graphene that depends on the frequency and chemical potential (μ_c).

Moreover, to evaluate the optical conductivity of the graphene nanodisk for investigating its plasmonic behavior, in the absence of an external magnetic field, we have used the simplified Kubo formula, neglecting the insignificant quantum size effects on the graphene plasmons [31], [53], [54]:

$$\begin{aligned}\sigma_g = {} & \frac{2e^2K_BT}{\pi\hbar^2}\frac{i}{\omega_0 + i2\pi\tau_g{}^{-1}}ln\left(2\,cosh\frac{\mu_c}{2K_BT}\right) \\ & + \frac{e^2}{4\hbar}\left\{\left[\frac{1}{2} + \frac{1}{\pi}\,arctan\left(\frac{\hbar\omega_0 - 2\mu_c}{2K_BT}\right)\right]\right. \\ & \left. - \frac{i}{2\pi}ln\left[\frac{(\hbar\omega_0 + 2\mu_c)^2}{(\hbar\omega_0 - 2\mu_c)^2 + 4K_BT}\right]\right\}\end{aligned} \tag{7}$$

where $\hbar$, e, and ω are the reduced Plank's constant, the electron charge, and the angular frequency, while $\tau_g = \mu_e\mu_c/eV_f{}^2$ is the carrier relaxation time in graphene with Fermi velocity of $V_F = 10^8\ cm.s^{-1}$and the mobility of $\mu_e = 10^4\ cm^2.V^{-1}.s^{-1}$.

The optical conductivity is mainly contributed by intraband transitions in the THz and far-infrared ranges and by interband carrier transitions in the visible and near-infrared ranges. The optical constants of graphene can be obtained with high accuracy by spectroscopy ellipsometry (SE). SE measures the phase shift difference and amplitude change between the incident and reflected light, and extracts the extinction coefficient (k) and refractive index (n) of graphene very accurately. Broadband optical properties of graphene have been measured by SE. There is a peak in both n and k at the energy around 1 eV. At lower energies (< 1 eV), both n and k decrease with reducing energy. At energies above 1 eV, with increasing the photon energy, the extinction coefficient k first decreases and then increases and peaks at 4.8 eV, while n becomes nearly a constant ($n \sim 2.9$) between energies 1 eV and 4 eV, and then decreases at higher energies [55]–[59].

Having the optical constants of graphene, other optical parameters such as absorbance, complex dielectric function, transmittance, and dynamic conductivity can be derived. The absorption of graphene is independent of frequency in the visible range and has a magnitude given by $\pi\alpha = 2.293\%$ per monolayer, where $\alpha = e^2/\hbar c$ denotes the fine-structure constant. Graphene shows a strong absorption peak around 4.8 eV due to the resonant excitons near the Van Hove singularity at the M point of the Brillouin zone. For energies below 1 eV, the absorbance decreases with reducing the energy. This can be attributed to the effects of the doping in the graphene film that cause a shift of the Fermi energy away from the Dirac point [55], [60].

IV. SIMULATION

To obtain the simulation results, we have considered a plane wave single-mode THz source with its electric field polarized along the x-direction that is illuminated on the surface of the graphene nanodisks at normal incidence. This incident light, at the resonance frequency, can effectively excite the LSPs on the surface of graphene nanodisks. The resulted LSPs field can trap the nanoparticles. The stable trapping of the nanoparticles can be determined using the depth of the potential well ($U \leqslant -10\ K_BT$). The potential energy can be obtained by integrating force (see (3)). On the other hand, as seen in (1) and (2), the force depends on the electromagnetic fields. To obtain the electromagnetic field distributions, Maxwell's equations are solved numerically, using the three-dimensional finite-difference time-domain (FDTD). For these calculations, the perfectly matched layers boundary condition along the z-direction have been utilized. The periodic boundary conditions along the x-, and y-directions are used. A mesh size of 1 nm is considered to achieve convergence of results to $\sim 1\%$, as its accuracy.

Having obtained the field distributions using Maxwell's equations, now, the average force exerted on a nanoparticle can be computed. Finally, the potential energy is calculated by integration of the force, and the trapping capability of the nanoparticles is considered.

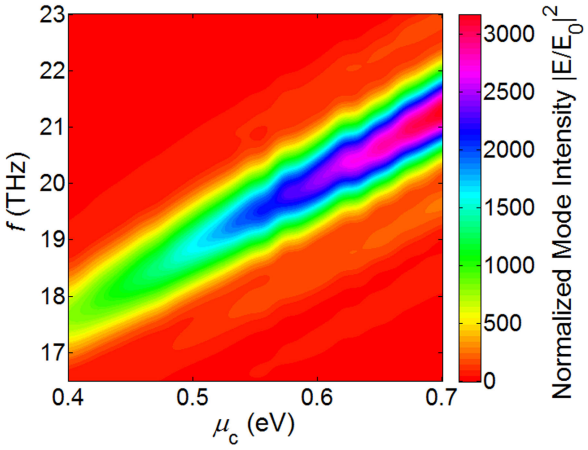

FIGURE 2. Normalized mode intensity profile versus f and μ_c on the surface of graphene nanodisk.

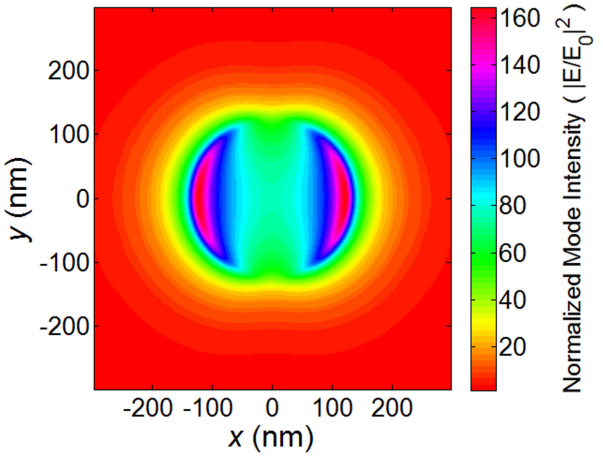

FIGURE 3. Normalized LSPs mode intensity in the x-y plane, and 10 nm above the surface of graphene nanodisk.

V. RESULTS AND DISCUSSIONS

To design an efficient tweezer system, first, we investigate the influence of chemical potential (μ_c) of the graphene nanodisk on the resonance frequency (f) and the corresponding mode intensity on its surface. For this purpose, as mentioned earlier, we assume a laser light is illuminated to a graphene nanodisk, as a system's unit cell, at normal incidence. The laser light is assumed to be a plane wave with linear polarization along the x-direction. The resonance frequency of the designed structure can be obtained using the circuit model and absorption spectra of graphene structures in THz spectra [38]–[40], [61], [62]. Given that there is a maximum excitation of plasmons at the absorption peak, hence the field intensity of plasmons is maximized at the resonance frequency. Fig. 2 shows the resonance frequency of the proposed structure versus the variations of the chemical potential of graphene nanodisk. As seen from this figure, the larger μ_c, the larger f, and the greater normalized mode intensity. Because the resonance frequency increases with the square root of the chemical potential ($f \propto {\mu_c}^{1/2}$) [38], [63]. In other words, as μ_c increases, the density of free electrons, and hence, the plasmon's density increases on the surface of graphene, enhancing the plasmons field intensity. Moreover, for a given μ_c, the mode intensity is maximized at a specific frequency, as the resonance frequency of LSPs. In addition to the chemical potential, the resonance frequency of graphene plasmons depends on the shape of the graphene nanostructure. For example, the resonance frequency of graphene nanoribbon and graphene nanodisk depends on the ribbon width and nanodisk diameter, respectively [64]–[66]. Generally, the resonance frequency of plasmons in graphene nanodisk depends on the chemical potential and diameter (D) of graphene nanodisk, and also the relative permittivities of its surrounding materials, i.e., ($f \propto \sqrt{\mu_c/(D(\varepsilon_w + \varepsilon_{substrate}))}$) [38], [63].

Now, considering a graphene nanodisk with a chemical potential of $\mu_c = 0.6$ eV, that is normally illuminated by a THz source polarized along x-direction of intensity $I = 19\ mW/\mu m^2$ and frequency of $f = 20$ THz, which centered about the resonance frequency of the doped graphene nanodisk with $\mu_c = 0.6$ eV (see Fig. 2), for excitation of LSPs on the nanodisk surface. It is worth noted that at the resonance frequency, the LSPs can be strongly excited, and the resulted plasmon's field intensity maximizes. Therefore, the resulting strong gradient force that is proportional to the intensity can efficiently trap the nanoparticles. In other frequencies, the LSPs of graphene nanodisk cannot be effectively excited, and the resulting plasmon's field is not intense enough to trap the particles. By solving Maxwell's equations, using the 3D FDTD, the field distribution on the surface of graphene and above it can be obtained. The origin of the coordinates is considered in the center of the nanodisk. Fig. 3 displays the profile of normalized mode intensity in the x-y plane ($z = 10$ nm) at the resonance frequency of $f = 20$ THz. The plasmon's field (E) is normalized to the field amplitude of the incident light (E_0). The field amplitude of the incident light is $E_0 = 2.85 \times 10^6$ (V/m), and the maximum amount of the LSPs field on the graphene surface is $E = 1.57 \times 10^8$ (V/m) that their values are smaller than the Coulomb field of the atoms. The Coulomb potential energy and the resulting Coulomb field in graphene are reported in the range of 3.6 eV to 17 eV and 1.5×10^{10} (V/m) to 7×10^{10} (V/m), respectively [67]–[69].

As shown in Fig. 3, the field intensity is non-uniform across the nanodisk (x-direction). It is maximum near the edges, i.e., the left and right sides of the graphene nanodisk where the intensity of the near field varies dramatically with positions. This can be attributed to the x-directional polarization of the incident light.

It should be noted that the plasmonic tweezers use the near-field of surface plasmons to trap the subwavelength particles. The surface plasmon is confined close to the metallic surface. It generates a high field intensity at the vicinity of the surface of graphene nanodisks. Therefore, the nanoparticles can be trapped if they move near the graphene surface. As the distance increases, the field evanesces through the fluidic

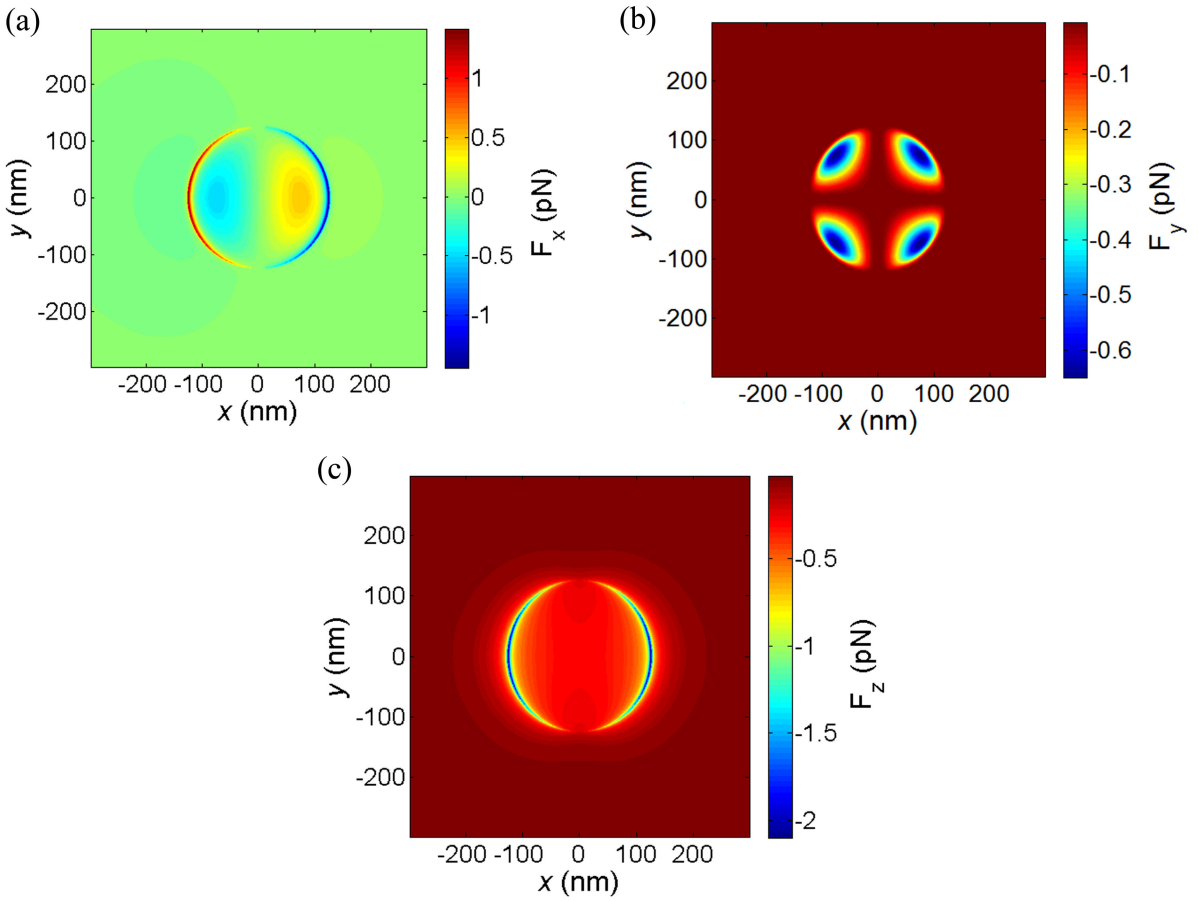

FIGURE 4. **(a,b) The transverse components, (c) The normal component, of the plasmonic forces exerted on a PS nanoparticle of $d = 12$ nm.**

and its intensity decreases. Hence, as will see in Fig. 5, the resulted force decreases with increasing the distance. Therefore, we consider $z = 10$ nm that the field intensity and the resulted force are strong enough to trap the nanoparticles.

Having obtained the field distribution on the surface of graphene nanodisk, using the 3D FDTD, we can now use the MST method to evaluate the average optical force exerted on the nearby nanoparticle by the corresponding LSPs field. Hence, we assume a spherical PS nanoparticle with a diameter of $d = 12$ nm that is suspended in the water solution, is located near the graphene nanodisk with a chemical potential of $\mu_c = 0.6$ eV, which may be realized by chemical or electrostatic doping [63]. As experimentally demonstrated in [41], the lithographically patterned multiple graphene nanodisks can connect to each other by quasi-1D graphene nanoribbons (GNRs). Then using two metal electrodes on both sides (in the x-direction) can apply the voltage to the graphene nanodisk via these GNRs.

Fig. 4 illustrates the components of optical force exerted on a PS nanoparticle with $d = 12$ nm. A distance of 10 nm is considered between the bottom of the PS nanoparticle and the graphene nanodisk. The transverse components of the optical force can trap the nanoparticles. As shown in Figs. 4 (a) and 4 (b), the value of the x-component of the optical force (F_x) is more than twice the y-component of the optical force (F_y), i.e., ($|F_{x,max}| = 1.4\ pN > |F_{y,max}| = 0.64\ pN$). Because the incident light is x-polarized and the LSPs highly excited in the x-direction and around the left and right sides of the nanodisk, as shown in Fig. 3. Therefore, the stronger field intensity causes the higher optical force, because optical force is proportional to the gradient of intensity (I), i.e., ($f \propto \nabla I$) [3], [50]. As shown in Fig. 4 (a), the F_x changes its sign near the edges of the nanodisk. Hence, the depth of the corresponding potential well in these positions can act as the trapping centers for nearby nanoparticles. The normal optical force component (F_z), Fig. 4 (c), which is stronger than the transverse components of the optical force, attracting the nanoparticles toward the graphene nanodisk surface. However, it can be balanced by various opposing forces, originating from the fluidic lift, thermophoresis, gravity, and electrostatic mechanisms, preventing the particles from sticking to the nanodisk surface [46].

Notably, the surface plasmons excited in graphene are confined much more strongly than those in conventional noble metals. Highly confined graphene's LSPs, because of the local field enhancements and the small spatial extensions, generate a strong evanescent near-field in the deep sub-wavelength area close to the surface of graphene. As the

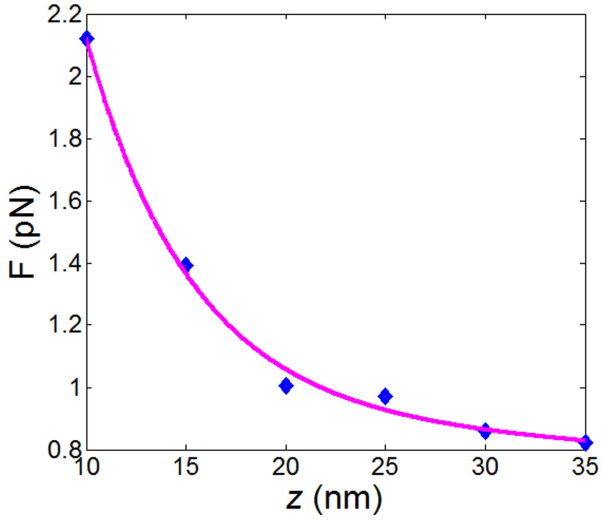

FIGURE 5. The magnitude of the plasmonic force exerted on a PS nanoparticle of $d = 12$ nm, as a function of distance above the surface of graphene nanodisk.

distance from the surface of graphene increases, the evanescent field attenuates through the medium. Hence, the gradient force decreases because the gradient force is proportional to the gradient of the field intensity.

Therefore, as shown in Fig. 5, strong optical near-field forces can be generated when the nanoparticles are located in the vicinity of a graphene nanodisk, and with increasing the distance from the surface of graphene, the force decreases. Furthermore, other research groups [43], [70] have experimentally demonstrated that the plasmonic tweezers can efficiently trap nanoparticles when they are within the plasmonic active nano-space, i.e., about 10–15 nm above the plasmonic surface. In this paper, the smallest nanoparticle that can be trapped within the plasmonic active nano-space is investigated. Hence, the trapping capability of the proposed structure at the distance of $z = 10$ nm from the surface of graphene nanodisk is considered. It is worth noted that when we have determined the size of the smallest nanoparticle that can be trapped, obviously larger particles can be trapped, too (because $f_{grad} \propto R^3$, as seen in (4)).

Using the transverse optical force components in the x-y plane, one can obtain the distribution of the potential energy, that determines the trapping capability of the tweezer. Fig. 6 (a) shows the transverse trapping potential (U_{xy}) experienced by a PS nanoparticle with a diameter of $d = 12$ nm. As shown in this figure, the potential energy at the edges of graphene nanodisk with $\mu_c = 0.6$ eV, is less than $-10\ k_BT$, satisfying the trapping condition. The threshold for stable optical trapping is $-10\ k_BT$. This potential depth necessity is considered for compensation of the stochastic kicks in the particle's Brownian motion to make stable trapping possible [71]. The optical force is proportional to the LSPs field intensity. Because the field intensity at the edges of graphene nanodisks maximizes (see Fig. 3), the corresponding gradient forces increase and the resulting potential energy is sufficiently deep enough to trap the PS nanoparticles near the

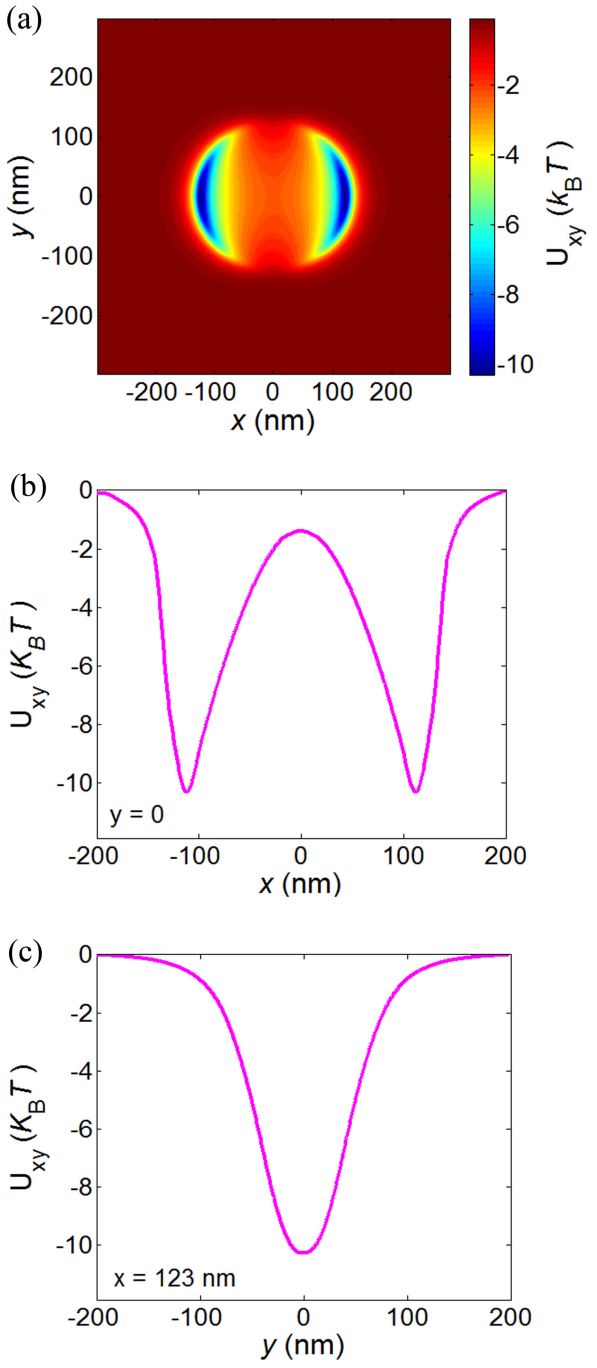

FIGURE 6. (a) Transverse potential energy (U_{xy}) sensed by a PS nanoparticle of $d = 12$ nm. (b,c) The variation of (U_{xy}) along $y = 0$ nm and $x = 123$ nm, respectively.

edges of the nanodisk. Fig. 6 (b) shows these two stable trapping points near the edges. Figs. 6 (b) and (c) illustrate the U_{xy} variations along $y = 0$ and $x = 123$ nm, respectively. As shown in these figures, the optical trap is tighter in the x-direction (FWHM $= 60$ nm) compared to the y-direction (FWHM $= 100$ nm), because of the stronger confinement of the electromagnetic field along the x-direction. Note that, the FWHM is the full-width at half maximum that is calculated for the Figs. 6 (b) and 6 (c).

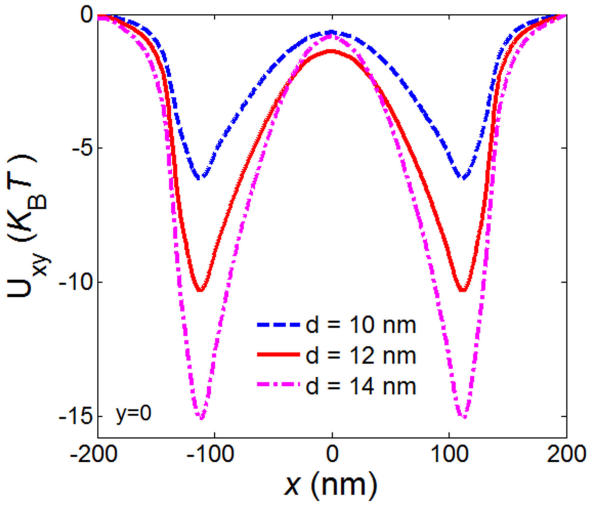

FIGURE 7. Variations of potential energy along $y = 0$, for PS nanoparticles with different diameters of $d = 10$ nm, 12 nm, and 14 nm.

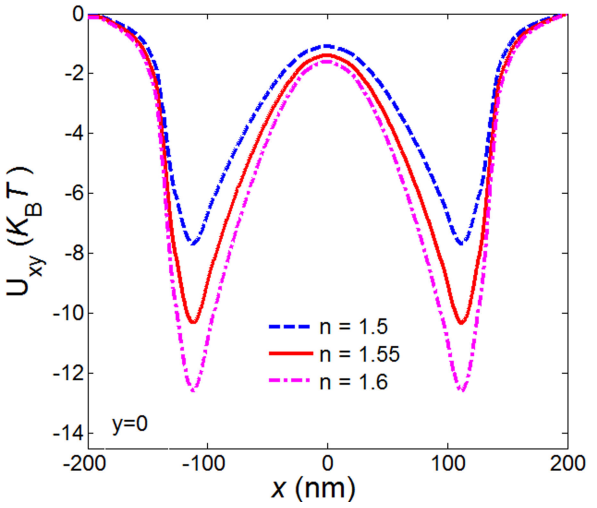

FIGURE 8. Profiles of potential energy for nanoparticles of the same diameters $d = 12$ nm but different refractive indices.

Using the same procedure as described above, we can obtain the potential energy for nanoparticles with different radii and refractive indices and investigate their trapping capabilities. Fig. 7 shows the U_{xy} variations along $y = 0$, for PS nanoparticles with different diameters. The gradient force is proportional to the nanoparticle diameter as $f_{grad} \propto (d/2)^3$ [3], [50]. Hence, with increasing the nanoparticle diameters, the gradient force enhances, and the resulting potential energy increases, as observed in Fig. 7. However, this potential energy is not deep enough, i.e., $|U_{xy}| < 10\,K_BT$, to trap the PS nanoparticles of diameter $d = 10$ nm. Therefore, graphene nanodisk with the chemical potential of 0.6 eV, can trap the PS nanoparticles with diameters of $d = 12$ nm and larger.

Another important parameter that affects the trapping functionality of the proposed system is the refractive index of nanoparticles. The potential energy sensed by nanoparticles with the same diameters of $d = 12$ nm and different refractive indices of $n = 1.5$, 1.55, and 1.6, is shown in Fig. 8. This figure reveals that as the particle refractive index increases, the depth of the potential well also increases. Moreover, it represents that the system-based graphene nanodisk with $\mu_c = 0.6$ eV is capable of trapping the nanoparticles of given diameters with refractive indices $n \geq 1.55$.

One of the most important properties of graphene plasmon is tunability. This is an interesting property of graphene that at an appropriate fixed incident laser power, as discussed in Fig. 2, the plasmon's field intensity can be controlled by changing the chemical potential of graphene. Fig. 9 shows the potential energy experienced by a PS nanoparticle with $d = 12$ nm that moving 10 nm above the surface of graphene nanodisk with different chemical potentials. For each chemical potential, the potential energy is obtained at the resonance frequency of graphene nanodisk. As shown in Fig. 2, it is worth noted that the resonance frequency increases with enhancing the chemical potential, because

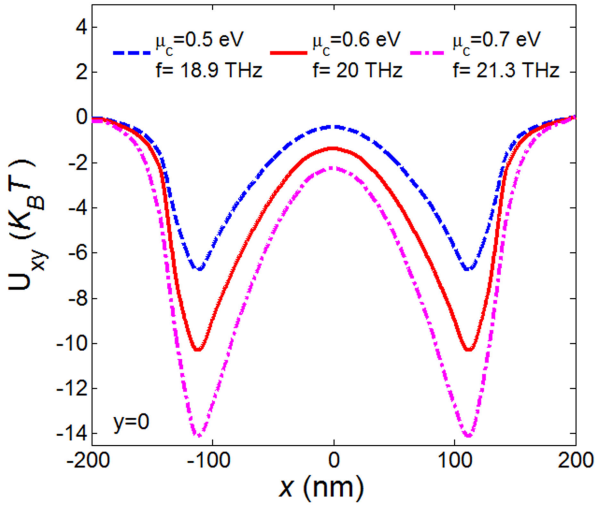

FIGURE 9. Variations of potential energy along $y = 0$, in different chemical potential of graphene nanodisk, for a PS nanoparticle with $d = 12$ nm.

$f \propto {\mu_c}^{1/2}$ [38], [63]. As represents in Fig. 9, with enhancing the chemical potential, the potential energy increases. Because with increasing the chemical potential, the free electrons density and hence the plasmon's density increases, enhancing the plasmon field intensity. Hence, the resulting gradient force increases as $f \propto \nabla I$ [3], [50]. Therefore, the resulting potential energy increases.

Moreover, the LSPs field of graphene nanodisk with a chemical potential of $\mu_c = 0.5$ eV, cannot trap the PS nanoparticles with $d = 12$ nm. Because the depth of the potential well is not deep enough to satisfy the stable trapping condition ($U < -10\,K_BT$). As shown in Fig. 10, our further investigations show that the graphene nanodisk with $\mu_c = 0.5$ eV can trap the PS nanoparticles with a diameter of $d = 18$ nm and larger. Also, the graphene nanodisk with $\mu_c = 0.7$ eV can trap the PS nanoparticles as small as 9.5 nm in diameter.

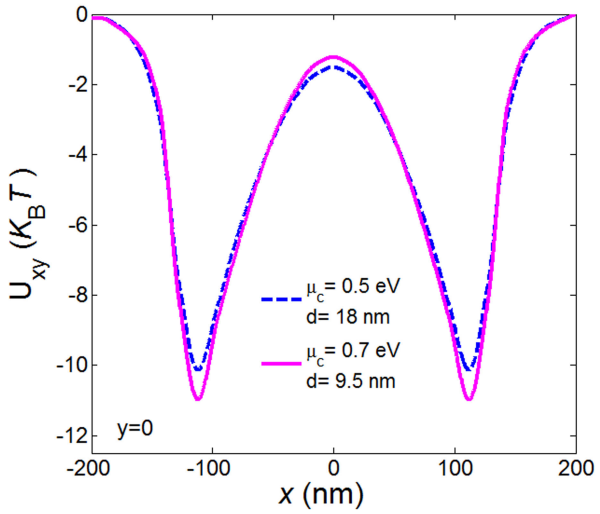

FIGURE 10. The potential energy sensed by PS nanoparticles of $d = 18$ nm and $d = 9.5$ nm, that are trapped by the LSPs field of graphene nanodisks with $\mu_c = 0.5$ eV and $\mu_c = 0.7$ eV, respectively.

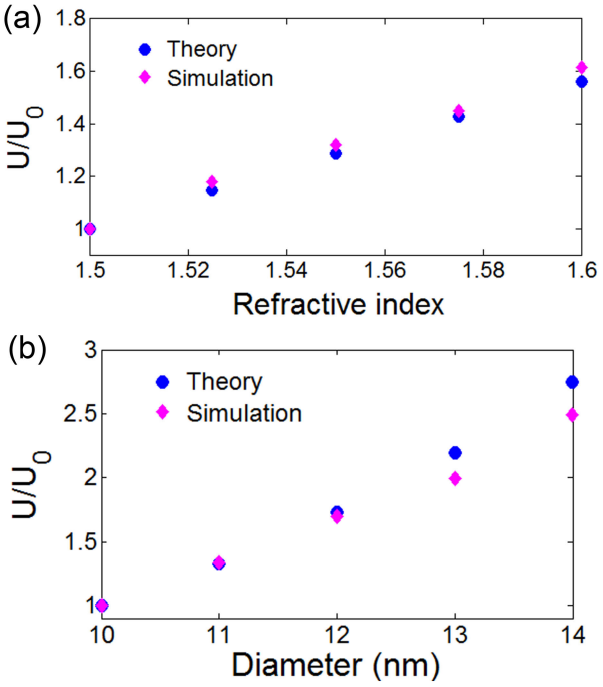

FIGURE 11. Normalized potential energy depth versus (a) refractive index of nanoparticle with $d = 12$ nm, (b) the diameter of PS nanoparticle.

Before calculating the trap stiffness and sensitivity of the proposed system, we compare our simulation results with theory. The trapping capability of the proposed system is determined by the depth of the potential well. Hence, the accuracy of the obtained potential energy is important for trapping the nanoparticles. Fig. 11 shows the simulation and theoretical results obtained for variations of the potential energy depth versus the nanoparticle diameter and its refractive index. Theoretical results are obtained using (5). Fig. 11 (a) shows the normalized potential energy depth (U/U_0) versus the refractive index of a dielectric particle with a given diameter of $d = 12$ nm. Where U_0 is the depth of potential well for a nanoparticle with $d = 12$ nm and a refractive index of $n = 1.5$. As shown in this figure, with enhancing the refractive index, the normalized potential depth increases. There is good agreement between the simulation results and theory. Fig. 11 (b) shows the normalized potential energy depth (U/U_0) versus the diameter of a PS nanoparticle. Where U_0 is the potential depth of a PS nanoparticle with a diameter of $d = 10$ nm. According to (5), the potential energy is proportional to $(d/2)^3$, and with increasing the nanoparticle's diameter, the potential energy increases, as shown in Fig. 11 (b). Also, the simulation results are almost in agreement with the theoretical results. A further agreement between simulation results and theory can be achieved if we reduce the mesh size as much as possible. However, this requires a computer system with higher specifications.

Using thermal fluctuations of the trapped nanoparticle in the potential well, the trap stiffness can be obtained through the equipartition theorem. For a nanoparticle in a harmonic potential well, the trap stiffness (k) can be evaluated using $(1/2)K_BT = (1/2)K < x^2 >$ [14], [72]–[74]. Where k_B is Boltzmann's constant, T is the temperature, and x is the displacement of the particle from its trapped equilibrium position. Using the potential energy profile (Figs. 6 (b) and 6 (c)), for a nanoparticle with $d = 12$ nm, the trapping stiffnesses at the minimum potential energy point are found to be $k_x = 53.48$ fN/nm along the x-direction and $k_y = 9.57$ fN/nm along the y-direction.

Similarly, the trap stiffnesses of the nanoparticles with different diameters of 10 nm, 12 nm, and 14 nm at the minimum potential (see Fig. 7) are obtained as $k_x = 32.02$ fN/nm, $k_x = 53.48$ fN/nm, and $k_x = 98.03$ fN/nm, respectively. Therefore, as the nanoparticle size increases, the trap stiffness increases.

It is worth noted that the trap stiffness of the proposed graphene nanodisk structure is higher than that of the reported plasmonic structures based on gold nanodisks, gold stripe, and gold nanohole array. On the other hand, it is approximately comparable to that of the coaxial plasmonic apertures, and Bull's Eye nanostructures. The reported values of trap stiffness for these plasmonic structures are as follows.

The trap stiffnesses of 0.03 fN/nm along x and 0.017 fN/nm along y for a 3.55 μm PS particle located above the gold nanodisk have been reported [73]. Using the surface plasmon polaritons on a gold stripe, a trapping stiffness of 1.7 fN/nm for 1 μm diameter PS particles was achieved [48]. The stiffness of 0.85 fN/nm was observed for trapping a 30 nm PS nanoparticle using a gold plasmonic nanohole array [75]. For a 10 nm diameter PS nanoparticle, the trap stiffnesses in the x and y directions of coaxial plasmonic apertures were reported about 105 fN/nm and 19.5 fN/nm, respectively [76]. The stiffnesses for a 200 nm diameter PS nanoparticle, trapped by a silver Bull's Eye nanostructure, in the x and y directions were achieved about 80 fN/nm and 10 fN/nm, respectively [77].

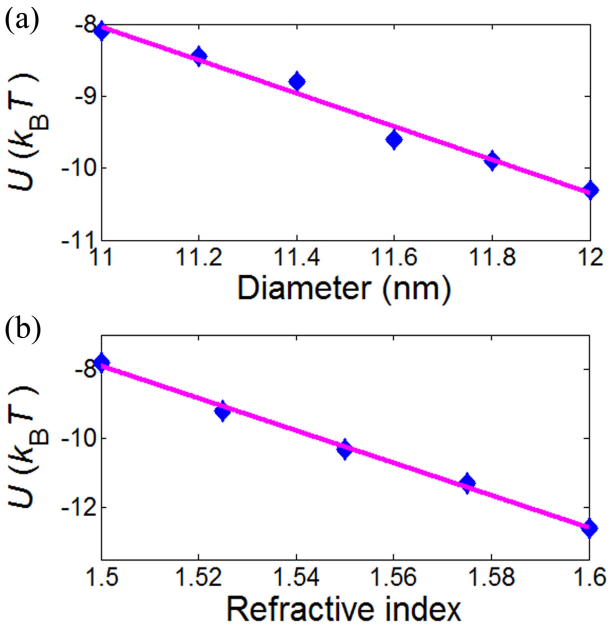

FIGURE 12. **Potential energy experienced by a nanoparticle versus its (a) diameter, and (b) refractive index.**

Finally, we investigate the trapping sensitivity in response to the minute changes in the nanoparticle diameter and its refractive index, which is the critical parameter of the proposed tweezer. Fig. 12 (a) reveals the variations in the potential energy versus the PS nanoparticle diameter. As shown in this figure, by slightly increasing the nanoparticle diameter, the depth of the potential energy increases with a nearly constant slope. From the slope of the linear fit of data presented in Fig. 12 (a), we can estimate the trapping sensitivity to a minute change in the nanoparticle diameter is $S_r = dU/dr \approx -2.25\ K_BT/nm$. Fig. 12 (b) illustrates the variations of the potential energy experienced by a nanoparticle of $d = 12$ nm versus its refractive index. Similarly, the nearly constant slope of the data shown in this figure reveals that the trapping sensitivity to a minute change in the nanoparticle refractive index is $S_n = dU/dn \approx -47\ K_BT/RIU$ per refractive index unit (RIU).

VI. CONCLUSION

In conclusion, we have designed a plasmonic tweezer system based on graphene's LSPs that can trap deep sub-wavelength nanoparticles. It is composed of a 2D array of graphene nanodisks. The LSPs on the surface of nanodisks are excited under normal illumination of the THz source. Graphene's LSPs, because of the local field enhancements and high confinement, generate the large field gradient in the deep sub-wavelength area around the resonance frequency. With an appropriate choice of the chemical potential of graphene nanodisks, the strong field intensity of LSPs can be obtained under the relatively low illumination intensity. Hence, the generated strong optical forces cause the deep potential wells to efficiently trap the nanoparticles. Numerical results show that the proposed structure with graphene nanodisks of $D = 250$ nm and $\mu_c = 0.6$ eV, can trap the PS nanoparticles of diameters $d \geq 12$ nm with an incident light intensity of 19 $mW/\mu m^2$ and the center resonance frequency of $f = 20$ THz. Furthermore, the proposed system with graphene nanodisk of $\mu_c = 0.7$ eV, and the resonance frequency of $f = 21.3$ THz, can trap the PS nanoparticle as small as 9.5 nm in diameter. The PS nanoparticles are trapped around the hot spots of the electromagnetic fields, near the edges of graphene nanodisk. Moreover, the trapping sensitivities of the designed tweezer for the minute changes in the nanoparticle diameter and its refractive index are $-2.25\ K_BT/nm$ and $-47\ K_BT/RIU$, respectively.

DISCLOSURES

The authors declare no conflicts of interest.

REFERENCES

[1] D. G. Grier, "A revolution in optical manipulation," *Nature*, vol. 424, pp. 810–816, Aug. 2003.
[2] K. Dholakia and P. Reece, "Optical micromanipulation takes hold," *Nano Today*, vol. 1, no. 1, pp. 18–27, Feb. 2006.
[3] D. Erickson, X. Serey, Y. F. Chen, and S. Mandal, "Nanomanipulation using near field photonics," *Lab Chip*, vol. 11, no. 6, pp. 995–1009, 2011.
[4] L. Novotny, R. X. Bian, and X. S. Xie, "Theory of nanometric optical tweezers," *Phys. Rev. Lett.*, vol. 79, no. 4, p. 645, 1997.
[5] O. J. F. Martin and C. Girard, "Controlling and tuning strong optical field gradients at a local probe microscope tip apex," *Appl. Phys. Lett.*, vol. 70, no. 6, pp. 705–707, Feb. 1997.
[6] K. Okamoto and S. Kawata, "Radiation force exerted on subwavelength particles near a nanoaperture," *Phys. Rev. Lett.*, vol. 83, no. 22, p. 4534, 1999.
[7] E. Ozbay, "Plasmonics: Merging photonics and electronics at nanoscale dimensions," *Science*, vol. 311, no. 5758, pp. 189–193, Jan. 2006.
[8] J. A. Schuller, E. S. Barnard, W. Cai, Y. C. Jun, J. S. White, and M. L. Brongersma, "Plasmonics for extreme light concentration and manipulation," *Nature Mater.*, vol. 9, no. 3, pp. 193–204, 2010.
[9] A. N. Grigorenko, N. W. Roberts, M. R. Dickinson, and Y. Zhang, "Nanometric optical tweezers based on nanostructured substrates," *Nature Photon.*, vol. 2, no. 6, pp. 365–370, Jun. 2008.
[10] M. Righini, P. Ghenuche, S. Cherukulappurath, V. Myroshnychenko, F. J. G. de Abajo, and R. Quidant, "Nano-optical trapping of Rayleigh particles and escherichia coli bacteria with resonant optical antennas," *Nano Lett.*, vol. 9, no. 10, pp. 3387–3391, Oct. 2009.
[11] W. Zhang, L. Huang, C. Santschi, and O. J. F. Martin, "Trapping and sensing 10 nm metal nanoparticles using plasmonic dipole antennas," *Nano Lett.*, vol. 10, no. 3, pp. 1006–1011, Mar. 2010.
[12] Y. Tsuboi, T. Shoji, N. Kitamura, M. Takase, K. Murakoshi, Y. Mizumoto, and H. Ishihara, "Optical trapping of quantum dots based on gap-mode-excitation of localized surface plasmon," *J. Phys. Chem. Lett.*, vol. 1, no. 15, pp. 2327–2333, Aug. 2010.
[13] Y. Pang and R. Gordon, "Optical trapping of 12 nm dielectric spheres using double-nanoholes in a gold film," *Nano Lett.*, vol. 11, no. 9, pp. 3763–3767, Sep. 2011.
[14] M. L. Juan, R. Gordon, Y. Pang, F. Eftekhari, and R. Quidant, "Self-induced back-action optical trapping of dielectric nanoparticles," *Nature Phys.*, vol. 5, no. 12, pp. 915–919, Dec. 2009.
[15] M. Ghorbanzadeh, S. Jones, M. K. Moravvej-Farshi, and R. Gordon, "Improvement of sensing and trapping efficiency of double nanohole apertures via enhancing the wedge plasmon polariton modes with tapered cusps," *ACS Photon.*, vol. 4, no. 5, pp. 1108–1113, May 2017.
[16] A. A. Khorami, M. K. Moravvej-Farshi, and S. Darbari, "Next-generation on-chip plasmonic tweezer with a built-in light source," *OSA Continuum*, vol. 3, no. 8, pp. 2044–2052, 2020.
[17] M. Righini, A. S. Zelenina, C. Girard, and R. Quidant, "Parallel and selective trapping in a patterned plasmonic landscape," *Nature Phys.*, vol. 3, no. 7, pp. 477–480, Jul. 2007.
[18] S. V. Boriskina, T. A. Cooper, L. Zeng, G. Ni, J. K. Tong, Y. Tsurimaki, Y. Huang, L. Meroueh, and G. Mahan, "Losses in plasmonics: From mitigating energy dissipation to embracing loss-enabled functionalities," *Adv. Opt. Photon.*, vol. 9, no. 4, pp. 775–827, Dec. 2017.

[19] K. B. Crozier, "Quo vadis, plasmonic optical tweezers?" *Light, Sci. Appl.*, vol. 8, no. 1, p. 35, Dec. 2019.
[20] M. Heidari, V. Faramarzi, Z. Sharifi, M. Hashemi, S. Bahadori-Haghighi, B. Janjan, and D. Abbott, "A high-performance TE modulator/TM-pass polarizer using selective mode shaping in a VO_2-based side-polished fiber," *Nanophotonics*, vol. 10, Aug. 2021, Art. no. 20210225.
[21] B. Janjan, M. Miri, D. Fathi, M. Heidari, and D. Abbott, "Hybrid Si_3N_4/VO_2 modulator thermally triggered by a graphene microheater," *IEEE J. Sel. Topics Quantum Electron.*, vol. 26, no. 5, pp. 1–6, Sep. 2020.
[22] E. H. Hwang and S. Das Sarma, "Dielectric function, screening, and plasmons in two-dimensional graphene," *Phys. Rev. B, Condens. Matter*, vol. 75, no. 20, May 2007, Art. no. 205418.
[23] L. Ju, B. Geng, J. Horng, C. Girit, M. Martin, Z. Hao, H. A. Bechtel, X. Liang, A. Zettl, and Y. R. Shen, "Graphene plasmonics for tunable terahertz metamaterials," *Nature Nanotechnol.*, vol. 6, no. 10, pp. 630–634, Sep. 2011.
[24] A. Vakil and N. Engheta, "Transformation optics using graphene," *Science*, vol. 332, no. 6035, pp. 1291–1294, 2011.
[25] J. Chen, M. Badioli, P. A. Gonzalez, S. Thongrattanasiri, F. Huth, J. Osmond, M. Spasenovic, A. Centeno, A. Pesquera, and P. Godignon, "Optical nano-imaging of gate-tunable graphene plasmons," *Nature*, vol. 487, no. 7405, pp. 77–81, Jul. 2012.
[26] M. Jablan, H. Buljan, and M. Soljačić, "Plasmonics in graphene at infrared frequencies," *Phys. Rev. B, Condens. Matter*, vol. 80, no. 24, Dec. 2009, Art. no. 245435.
[27] F. H. L. Koppens, D. E. Chang, and F. J. G. de Abajo, "Graphene plasmonics: A platform for strong light-matter interactions," *Nano Lett.*, vol. 11, pp. 3370–3377, Jul. 2011.
[28] L. Wang, M. Bie, W. Cai, X. Zhang, and J. Xu, "Graphene plasmonic Tamm states with ultracompact footprint," *Phys. Rev. Appl.*, vol. 12, no. 2, Aug. 2019, Art. no. 024057.
[29] A. A. Khorami, M. K. M. Farshi, and S. Darbari, "Ultralow-power electrically activated lab-on-a-chip plasmonic tweezers," *Phys. Rev. Appl.*, vol. 13, no. 2, Feb. 2020, Art. no. 024072.
[30] M. Heidari and V. Ahmadi, "Graphene-based mid-infrared plasmonic isolator with multimode interferometer," *Opt. Lett.*, vol. 45, no. 20, pp. 5764–5767, 2020.
[31] M. Ghorbanzadeh, S. Darbari, and M. K. Moravvej-Farshi, "Graphene-based plasmonic force switch," *Appl. Phys. Lett.*, vol. 108, no. 11, Mar. 2016, Art. no. 111105.
[32] M. Samadi, S. Darbari, and M. K. Moravvej-Farshi, "Numerical investigation of tunable plasmonic tweezers based on graphene stripes," *Sci. Rep.*, vol. 7, no. 1, Dec. 2017, Art. no. 14533.
[33] M. M. Abbasi, S. Darbari, and M. K. Moravvej-Farshi, "Tunable plasmonic force switch based on graphene nano-ring resonator for nanomanipulation," *Opt. Exp.*, vol. 27, no. 19, pp. 26648–26660, 2019.
[34] A. A. Balandin, S. Ghosh, W. Bao, I. Calizo, D. Teweldebrhan, F. Miao, and C. N. Lau, "Superior thermal conductivity of single-layer graphene," *Nano Lett.*, vol. 8, no. 3, pp. 902–907, 2008.
[35] J.-D. Kim and Y.-G. Lee, "Graphene-based plasmonic tweezers," *Carbon*, vol. 103, pp. 281–290, Jul. 2016.
[36] J. Zhang, W. Liu, Z. Zhu, X. Yuan, and S. Qin, "Towards nano-optical tweezers with graphene plasmons: Numerical investigation of trapping 10-nm particles with mid-infrared light," *Sci. Rep.*, vol. 6, no. 1, Dec. 2016, Art. no. 38086.
[37] X. Xu, L. Shi, Y. Liu, Z. Wang, and X. Zhang, "Enhanced optical gradient forces between coupled graphene sheets," *Sci. Rep.*, vol. 6, no. 1, Sep. 2016, Art. no. 28568.
[38] Z. Fang, Y. Wang, A. E. Schlather, Z. Liu, P. M. Ajayan, F. J. G. de Abajo, P. Nordlander, X. Zhu, and N. J. Halas, "Active tunable absorption enhancement with graphene nanodisk arrays," *Nano Lett.*, vol. 14, no. 1, pp. 299–304, 2014.
[39] J. Zhang, Z. Zhu, W. Liu, X. Yuan, and S. Qin, "Towards photodetection with high efficiency and tunable spectral selectivity: Graphene plasmonics for light trapping and absorption engineering," *Nanoscale*, vol. 7, no. 32, pp. 13530–13536, 2015.
[40] L. Zundel and A. Manjavacas, "Spatially resolved optical sensing using graphene nanodisk arrays," *ACS Photon.*, vol. 4, no. 7, pp. 1831–1838, Jul. 2017.
[41] Q. Guo, R. Yu, C. Li, S. Yuan, B. Deng, F. J. García de Abajo, and F. Xia, "Efficient electrical detection of mid-infrared graphene plasmons at room temperature," *Nature Mater.*, vol. 17, no. 11, pp. 986–992, Nov. 2018.
[42] M. L. Juan, M. Righini, and R. Quidant, "Plasmon nano-optical tweezers," *Nature Photon.*, vol. 5, no. 6, p. 349, 2011.
[43] B. J. Roxworthy and K. C. Toussaint, "Femtosecond-pulsed plasmonic nanotweezers," *Sci. Rep.*, vol. 2, no. 1, p. 660, Dec. 2012.
[44] A. Dalili, E. Samiei, and M. Hoorfar, "A review of sorting, separation and isolation of cells and microbeads for biomedical applications: Microfluidic approaches," *Analyst*, vol. 144, no. 1, pp. 87–113, 2019.
[45] J. Kim and J. H. Shin, "Stable, free-space optical trapping and manipulation of sub-micron particles in an integrated microfluidic chip," *Sci. Rep.*, vol. 6, no. 1, Sep. 2016, Art. no. 33842.
[46] M. Ghorbanzadeh, M. K. Moravvej-Farshi, and S. Darbari, "Designing a plasmonic optophoresis system for trapping and simultaneous sorting/counting of micro- and nano-particles," *J. Lightw. Technol.*, vol. 33, no. 16, pp. 3453–3460, Aug. 15, 2015.
[47] J. Xiao, H. Zheng, Y. Sun, and Y. X. Yao, "Bipolar optical forces on dielectric and metallic nanoparticles by an evanescent wave," *Opt. Lett.*, vol. 35, no. 7, pp. 962–964, 2010.
[48] K. Wang, E. Schonbrun, P. Steinvurzel, and K. B. Crozier, "Scannable plasmonic trapping using a gold stripe," *Nano Lett.*, vol. 10, no. 9, pp. 3506–3511, Sep. 2010.
[49] A. A. Saleh, S. Sheikhoelislami, S. Gastelum, and J. A. Dionne, "Grating-flanked plasmonic coaxial apertures for efficient fiber optical tweezers," *Opt. Exp.*, vol. 24, no. 18, pp. 20593–20603, 2016.
[50] K. Svoboda and S. M. Block, "Optical trapping of metallic Rayleigh particles," *Opt. Lett.*, vol. 19, no. 13, pp. 930–932, 1994.
[51] X. Wang, X. Xia, J. Wang, F. Zhang, Z.-D. Hu, and C. Liu, "Tunable plasmonically induced transparency with unsymmetrical graphene-ring resonators," *J. Appl. Phys.*, vol. 118, no. 1, Jul. 2015, Art. no. 013101.
[52] M. Heidari and V. Ahmadi, "Design and analysis of a graphene magneto-plasmon waveguide for plasmonic mode switch," *IEEE Access*, vol. 7, pp. 43406–43413, 2019.
[53] L. A. Falkovsky and A. A. Varlamov, "Space-time dispersion of graphene conductivity," *Eur. Phys. J. B*, vol. 56, no. 4, pp. 281–284, Apr. 2007.
[54] S. Thongrattanasiri, A. Manjavacas, and F. J. G. de Abajo, "Quantum finite-size effects in graphene plasmons," *ACS Nano*, vol. 6, no. 2, pp. 1766–1775, 2012.
[55] W. Li, G. Cheng, Y. Liang, B. Tian, X. Liang, L. Peng, A. R. H. Walker, D. J. Gundlach, and N. V. Nguyen, "Broadband optical properties of graphene by spectroscopic ellipsometry," *Carbon*, vol. 99, pp. 348–353, Apr. 2016.
[56] J. W. Weber, V. E. Calado, and M. C. M. van de Sanden, "Optical constants of graphene measured by spectroscopic ellipsometry," *Appl. Phys. Lett.*, vol. 97, no. 9, Aug. 2010, Art. no. 091904.
[57] A. Matković, U. Ralević, M. Chhikara, M. M. Jakovljević, D. Jovanović, G. Bratina, and R. Gajić, "Influence of transfer residue on the optical properties of chemical vapor deposited graphene investigated through spectroscopic ellipsometry," *J. Appl. Phys.*, vol. 114, no. 9, Sep. 2013, Art. no. 093505.
[58] F. J. Nelson, V. K. Kamineni, T. Zhang, E. S. Comfort, J. U. Lee, and A. C. Diebold, "Optical properties of large-area polycrystalline chemical vapor deposited graphene by spectroscopic ellipsometry," *Appl. Phys. Lett.*, vol. 97, no. 25, Dec. 2010, Art. no. 253110.
[59] M. Bruna and S. Borini, "Optical constants of graphene layers in the visible range," *Appl. Phys. Lett.*, vol. 94, no. 3, Jan. 2009, Art. no. 031901.
[60] K. F. Mak, M. Y. Sfeir, Y. Wu, C. H. Lui, J. A. Misewich, and T. F. Heinz, "Measurement of the optical conductivity of graphene," *Phys. Rev. Lett.*, vol. 101, no. 19, Nov. 2008, Art. no. 196405.
[61] S. Barzegar-Parizi, B. Rejaei, and A. Khavasi, "Analytical circuit model for periodic arrays of graphene disks," *IEEE J. Quantum Electron.*, vol. 51, no. 9, pp. 1–7, Sep. 2015.
[62] M. Biabanifard, A. Arsanjani, M. S. Abrishamian, and D. Abbott, "Tunable terahertz graphene-based absorber design method based on a circuit model approach," *IEEE Access*, vol. 8, pp. 70343–70354, 2020.
[63] Z. Fang, S. Thongrattanasiri, A. Schlather, Z. Liu, L. Ma, Y. Wang, P. M. Ajayan, P. Nordlander, N. J. Halas, and F. J. G. de Abajo, "Gated tunability and hybridization of localized plasmons in nanostructured graphene," *ACS Nano*, vol. 7, pp. 2388–2395, Feb. 2013.
[64] X. Luo, T. Qiu, W. Lu, and Z. Ni, "Plasmons in graphene: Recent progress and applications," *Mater. Sci. Eng., R, Rep.*, vol. 74, no. 11, pp. 351–376, Nov. 2013.

[65] F. J. G. de Abajo, "Graphene plasmonics: Challenges and opportunities," *ACS Photon.*, vol. 1, pp. 135–152, Feb. 2014.
[66] P.-Y. Chen, C. Argyropoulos, M. Farhat, and J. S. Gomez-Diaz, "Flatland plasmonics and nanophotonics based on graphene and beyond," *Nanophotonics*, vol. 6, no. 6, pp. 1239–1262, Apr. 2017.
[67] T. O. Wehling, E. Şaşioğlu, C. Friedrich, A. I. Lichtenstein, M. I. Katsnelson, and S. Blügel, "Strength of effective Coulomb interactions in graphene and graphite," *Phys. Rev. Lett.*, vol. 106, no. 23, Jun. 2011, Art. no. 236805.
[68] P. V. Buividovich and M. I. Polikarpov, "Monte Carlo study of the electron transport properties of monolayer graphene within the tight-binding model," *Phys. Rev. B, Condens. Matter*, vol. 86, no. 24, Dec. 2012, Art. no. 245117.
[69] M. V. Ulybyshev, P. V. Buividovich, M. I. Katsnelson, and M. I. Polikarpov, "Monte Carlo study of the semimetal-insulator phase transition in monolayer graphene with a realistic interelectron interaction potential," *Phys. Rev. Lett.*, vol. 111, no. 5, Jul. 2013, Art. no. 056801.
[70] Y. Tanaka, S. Kaneda, and K. Sasaki, "Nanostructured potential of optical trapping using a plasmonic nanoblock pair," *Nano Lett.*, vol. 13, no. 5, pp. 2146–2150, May 2013.
[71] A. Ashkin, J. M. Dziedzic, J. E. Bjorkholm, and S. Chu, "Observation of a single-beam gradient force optical trap for dielectric particles," *Opt. Lett.*, vol. 11, no. 5, pp. 288–290, 1986.
[72] X. Han, V. G. Truong, and S. N. Chormaic, "Efficient microparticle trapping with plasmonic annular apertures arrays," *Nano Futures*, vol. 2, no. 3, Aug. 2018, Art. no. 035007.
[73] M. Righini, G. Volpe, C. Girard, D. Petrov, and R. Quidant, "Surface plasmon optical tweezers: Tunable optical manipulation in the femtonewton range," *Phys. Rev. Lett.*, vol. 100, no. 18, May 2008, Art. no. 186804.
[74] K. C. Neuman and S. M. Block, "Optical trapping," *Rev. Sci. Instrum.*, vol. 75, no. 9, pp. 2787–2809, Sep. 2004.
[75] X. Han, V. G. Truong, P. S. Thomas, and S. N. Chormaic, "Sequential trapping of single nanoparticles using a gold plasmonic nanohole array," *Photon. Res.*, vol. 6, no. 10, pp. 981–986, 2018.
[76] A. A. E. Saleh and J. A. Dionne, "Toward efficient optical trapping of sub-10-nm particles with coaxial plasmonic apertures," *Nano Lett.*, vol. 12, no. 11, pp. 5581–5586, Nov. 2012.
[77] P. R. Huft, J. D. Kolbow, J. T. Thweatt, and N. C. Lindquist, "Holographic plasmonic nanotweezers for dynamic trapping and manipulation," *Nano Lett.*, vol. 17, no. 12, pp. 7920–7925, Dec. 2017.

ALI ASGHAR KHORAMI was born in Jahrom, Shiraz, Fars, Iran, in 1986. He received the M.Sc. degree in photonics-electronics from Tabriz University, Tabriz, Iran, in 2010, and the Ph.D. degree in nanotechnology-nanoelectronics from Tarbiat Modares University, Tehran, Iran, in 2020.

He is currently a Researcher with the Nanoelectronics Group, Tarbiat Modares University (TMU). His research interests include nanoelectronic, nanophotonic, plasmonic, tweezer, and graphene and 2D materials-based photonic devices.

MOHAMMAD MAHDI ABBASI received the B.Sc. degree in electrical engineering-electronics from Boroujerd University, Lorestan, Iran, in 2008, the M.Sc. degree in nanotechnology engineering-nanoelectronic from Tabriz University, in 2012, and the Ph.D. degree in nanotechnology-nanoelectronics from Tarbiat Modares University (TMU), Tehran, Iran, in 2019.

He is currently a Researcher with the Nanoelectronics Group, TMU. His research interests include nanoelectronic, nanophotonic, plasmonic tweezers, ring resonator, and graphene and 2D materials-based plasmonic.

ATHAR SADAT JAVANMARD received the B.Sc. degree in biology from Shiraz University, Shiraz, Iran, in 2004, the M.Sc. degree in cell and molecular biology from Azarbaijan Shahid Madani University, Iran, in 2008, and the Ph.D. degree in cell and molecular biology from Ferdowsi University of Mashhad, Iran, in 2018.

She is currently an Assistant Professor with the Department of Biology, Yasouj University, Iran. Her current research interests include biotechnology of enzymes and nanobiotechnology.